High-Temperature Atomic Force Microscopy of Normal Alkane $C_{60}H_{122}$ Films on Graphite

Sergei N. Magonov* and Natalya A. Yerina

Digital Instruments/Veeco Metrology Group, 112 Robin Hill Road, Santa Barbara, California 93117

Received July 22, 2002. In Final Form: October 8, 2002

The morphology of ultrathin films of normal alkane $C_{60}H_{122}$ has been examined with atomic force microscopy at temperatures between 25 and 150 °C. The films were prepared by spin-casting of diluted alkane solutions on graphite. Epitaxial alkane layers, which are formed directly on the substrate surface, are characterized by lamellar morphology. A lamellar width of 7.5 nm corresponds to the length of the extended $C_{60}H_{122}$ molecule. A topmost layer was formed of nanocrystals up to 10 nm in height. The nanocrystals consist of multiple layers of $C_{60}H_{122}$ lamellae, which are oriented parallel to the substrate. Imaging of the alkane films at elevated temperatures has revealed that the nanocrystals melted around 95 °C, while the epitaxial layers have been observed at temperatures up to 140 °C. In some locations, a spontaneous reorientation of alkane lamellae has been noticed at temperatures in the 130−140 °C range.

Introduction

Self-assembly of organic molecules on various substrates is an important subject in both academic and industrial research. Characterization of organic layers on substrates has advanced with the introduction of scanning tunneling microscopy (STM) and atomic force microscopy (AFM).[1] Both methods provide high-resolution imaging of surface structures and can be used for studies not only in ultrahigh vacuum but also at ambient conditions and under liquid. Initially, STM was applied to the study of molecular ordering at liquid−solid interfaces, and the images of alkylcyanobiphenyls,[2] normal alkanes C_nH_{2n+1},[3] and cyclic alkanes C_nH_{2n}[4] deposited on graphite have revealed the molecular order of these adsorbates. This epitaxial order is governed by an alignment of extended alkane chains along the main lattice directions of the substrate.[5] The orientation of the zigzag plane of the alkane molecules (all-trans conformation) is not necessarily fixed: the zigzag backbone either lies flat on the substrate or is perpendicular to it. A tumbling of alkane molecules between these orientations of its all-trans backbone has been noticed in STM images[6] and in a neutron scattering study.[7]

Since in STM a tip−sample current is the probing interaction, STM application requires at least a small sample conductivity, which is detectable only for one or a few layers of organic material (which is an insulator in bulk) lying on a conducting substrate. What is detected in the STM images of alkanes on graphite is primarily an electron density of the top H-atoms of alkanes, which contribute to a conducting band of the alkane/graphite system.[4] Further interest in the STM of alkanes deposited on graphite is related to various theoretical and practical aspects of identification of functional groups in functionalized[8] and primary substituted alkanes.[9]

There is another issue concerning STM imaging on samples with poor conductivity. Strong tip−sample force interactions, which are common for ambient-condition STM,[10] might prohibit a stable imaging of the single-lying organic layer. Therefore, STM images of alkanes and alkylcyanobiphenyls are usually recorded within the droplet of the saturated alkane solution. It has been shown that an STM tip penetrates through a poorly ordered adsorbate layer before reaching the ordered molecular layer on the substrate.[11] Lamellar ordering of alkanes (such as the one granted by alkane registry to graphite) ensures some mechanical stability of these layers. Furthermore, at the conditions of a saturated alkane solution, the epitaxial layer restores its integrity when it has been occasionally damaged by the STM tip. The latter circumstance might explain why STM imaging of single alkane layers on graphite (without alkane material above the single layer) has not been reported (at least to the best of our knowledge).

The requirement of sample conductivity for visualization of organic adsorbates was eliminated with the introduction of AFM.[12] Nowadays, this method is routinely applied to studies of organic layers of different thicknesses on various substrates. In the beginning, AFM studies of organic layers were performed in the contact mode, and the images of ordered organic layers showed their molecular-scale lattices.[13] One should be aware that a substantial shearing force, which is applied by a scanning probe to a surface layer in the contact mode, induces an undesirable disturbance of molecules and their positions on a substrate.

* Corresponding author. Phone: 805-9672700 ext 2229. Fax: 805-9677717. E-mail: sergei@di.com.

(1) (a) Binnig, G.; Rohrer, H.; Gerber, Ch.; Weibel, E. *Phys. Rev. Lett.* **1982**, *49*, 57. (b) Binnig, G.; Quate, C.; Gerber, Ch. *Phys. Rev. Lett.* **1986**, *56*, 930. (c) *Procedures in Scanning Probe Microscopies*; Colton, R. J., Engel, A., Frommer, J. E., Gaub, H. E., Gewirth, A. A., Guckenberger, R., Rabe, J., Heckl, W. M., Parkinson, B., Eds.; J. Wiley & Sons: New York, 1998.

(2) Foster, J.; Frommer, J. *Nature* **1988**, *60*, 1418.

(3) McGonigal, G. C.; Bernhardt, R. H.; Thomson, D. J. *Appl. Phys. Lett.* **1990**, *57*, 28.

(4) Liang, W.; Whangbo, M.-H.; Wawkuschewski, A.; Cantow, H.-J.; Magonov, S. N. *Adv. Mater.* **1993**, *5*, 817.

(5) Groszek, A. *Proc. R. Soc. London, Ser. A* **1970**, *314*, 473.

(6) Wawkushewski, A.; Cantow, H.-J.; Magonov, S. N.; Möller, M.; Liang, W.; Whangbo, M.-H. *Adv. Mater.* **1993**, *5*, 821.

(7) Hertwig, K. W.; Matthies, B.; Taub, H. *Phys. Rev. Lett.* **1995**, *75*, 3154.

(8) Claypool, C. L.; Faglioni, F.; Goddard, W. A., III; Gray, H. B.; Lewis, N. S.; Markus, R. A. *J. Phys. Chem. B* **1997**, *101*, 5978.

(9) Cyr, D. M.; Venkataram, B.; Flynn, G. W.; Black, A.; Whitesides, G. M. *J. Phys. Chem.* **1996**, *100*, 13747.

(10) (a) Soler, J. M.; Baro, A. M.; Garcia, N.; Rohrer, H. *Phys. Rev. Lett.* **1986**, *57*, 444. (b) Mamin, H. J.; Ganz, E.; Abraham, D. W.; Thompson, R. E.; Clarke, J. *Phys. Rev. B* **1986**, *34*, 9015.

(11) Wawkuschewski, A.; Cantow, H.-J.; Magonov, S. N. *Langmuir* **1993**, *9*, 2778.

(12) Binnig, G.; Quate, C.; Gerber, Ch. *Phys. Rev. Lett.* **1986**, *56*, 930.

(13) Tuzov, I.; Crämer, K.; Pfannemüller, B.; Kreutz, W.; Magonov, S. N. *Adv. Mater.* **1995**, *7*, 656.

10.1021/la0206615 CCC: $25.00
Published on Web 01/11/2003

The lateral tip−sample forces are practically eliminated in tapping mode.[14] This allows AFM imaging of soft materials, weakly bonded organic layers, and individual macromolecules.[15] Further advances in AFM applications involve studies at elevated temperatures (up to 250 °C).[16] Such studies are useful for in situ monitoring of polymer crystallization[17] and for exploring the mobility and adhesion of individual macromolecules on different substrates.[18] One can expect that studies of organic thin layers in tapping mode at elevated temperatures will provide advanced information about structural changes in such systems and complement the earlier attempts of the temperature studies in contact mode.[19]

AFM studies of alkane adsorbates on graphite are less common than those made with STM. In this letter, we present new results of AFM studies of normal alkane $C_{60}H_{122}$ layers on graphite at different temperatures. It was found that the alkane layers, which are formed on graphite, consist of flat-lying lamellae. The lamellar width of 7.5 nm corresponds to the length of extended $C_{60}H_{122}$ molecules, which are aligned along the main crystallographic directions of the graphite. The epitaxially arranged lamellae decorate the graphite grains that arise from the crystal defects. Nanocrystals of $C_{60}H_{122}$ alkanes, which are made up of lamellar layers, have been formed on top of the epitaxial layers. The nanocrystals melted around 95 °C, consistent with the melting temperature of bulk $C_{60}H_{122}$ crystals. The epitaxial layers are more thermally stable; they have been observed at temperatures up to 140 °C. A rearrangement of the lamellar orientation has been detected in some of the $C_{60}H_{122}$ epitaxial domains at 130−140 °C.

Experimental Section

Sample Preparation. A commercial sample of $C_{60}H_{122}$ alkane (Sigma-Aldrich) was used in our studies. According to the manufacturer, the melting temperature of this alkane is 94−96 °C. Highly ordered pyrolitic graphite was obtained from NTMDT (Zelenograd, Russia). A fresh surface of graphite was prepared by its cleavage with an adhesive tape. This procedure opens a clean atomically flat surface with a number of defects such as grain boundaries and steps even for graphite samples of high grade. Therefore, in many cases adsorbate layers decorate these surface features. Ultrathin layers of $C_{60}H_{122}$ on graphite were prepared using spin-casting, in which a droplet of a diluted solution of the alkane in xylene (0.01−0.001 g/L) was deposited on a freshly cleaved surface of graphite. Spin-casting was performed with a spin-coater, Speedline Technologies model P6204, at 2000 rpm.

AFM Measurements. AFM measurements were carried out with a scanning probe microscope, MultiMode Nanoscope IIIa (Digital Instruments), equipped with a J-scanner that allows imaging of surface areas up to 200 microns. For *XY* calibration in the sub-100-nm scale, the scanner was used in the contact mode imaging of the *ab*-plane of the organic charge-transfer salt crystal of TTF−TCNQ (TTF = tetrathiafulvalene, TCNQ = tetracyanoquinodimethane), which has the following crystallographic parameters: $a = 12.298$ Å, $b = 3.819$ Å, $c = 18.468$ Å, $\alpha = g = 90°$, $\beta = 104.46°$.[20] Imaging of atomic-scale lattices with the J-scanner does not provide well-resolved patterns; however, a linear structure with a periodicity of 1.3 nm was clearly observed. Thus we obtained a ∼1.3/1.23 adjustment coefficient for lateral measurements, which is approximately the same for both *X*- and *Y*-directions. To make adjustments in the *z*-calibration, we have measured surface steps, which according to the crystallographic data should be 0.895 nm. A deviation of the *z*-calibration was within 10%, and it was corrected appropriately.

For heating studies, we have used a commercial thermal accessory of the MultiMode microscope.[16] Both the sample and the probe are heated in this accessory. The dual action provides fast and precise heating (±1 °C as judged by melting of an In standard) of a surface area scanned by the probe. It also ensures stability of tapping mode imaging at elevated temperatures. Tapping mode was used in most experiments. Noncoated Si etched probes (length ∼225 microns; width ∼40 microns) with a stiffness of 1−3 N/m (resonance frequency, 50−60 kHz) from Nanosensors (Germany) and Mikromasch (Estonia) were applied in our measurements. For imaging of ultrathin $C_{60}H_{122}$ layers, scanning rates up to 20 Hz were applied.

In our AFM studies with tapping mode, we simultaneously recorded height and phase images. The height of the alkane nanocrystals was estimated with respect to the adsorbed layers using cross-sectional profiles or height histograms of bearing analysis. Both procedures are included in the analysis software provided by the microscope manufacturer. The value of phase imaging is primarily recognized in compositional mapping of heterogeneous materials,[17] yet it also enhances fine details of the surface order of the alkane samples. Optimization of the tip−sample force appeared to be the most important issue of AFM imaging of the alkanes at different temperatures. Room-temperature imaging of the surface morphology of the alkane adsorbates was performed at relatively low tip-force conditions (*light tapping*): the free-oscillating amplitude $A_0 = 20-30$ nm, and the set-point amplitude $A_{sp} = 15-20$ nm. At elevated temperatures (100−150 °C), when nearly all adsorbate is melted, *light tapping* imaging is less stable because the tip sticks to the melted material. In this case, imaging with $A_0 = 50-60$ nm and $A_{sp} = 5-6$ nm was most useful for visualization of the epitaxial alkane order at the melt−substrate interface. At such conditions, the probe penetrates through a topmost layer of the alkane melt and images the epitaxial layer. Similar AFM observations of the subsurface structures are known for other materials with rubbery or soft topmost surface layers. For example, imaging of poly(styrene)-*block*-polybutadiene-*block*-poly(styrene) film at elevated forces reveals the microphase-separated pattern, which is hidden underneath the lamella-thick surface layer of polybutadiene.[21] In a recent paper,[22] it was shown that the top of the polymer adsorbate on graphite might consist of a poorly ordered material. The AFM probe penetrated the poorly organized overlayer to come into contact with rigid and ordered self-assemblies of macromolecules on the substrate.

Results

The typical morphology of the spin-cast $C_{60}H_{122}$ layer on graphite is shown in Figure 1a. Multiple steps of a graphite substrate are decorated with flat nanocrystals. The latter are recognized by mostly regular bright patterns separated by dark borders. The nanocrystals in Figure 1a form large domains, yet single-lying nanocrystals such as the one seen in Figure 1c have also been found. The phase image in Figure 1b "magnifies" one of the locations in Figure 1a and reveals surface features of three neighboring crystals. Differently oriented strips 7.5 nm in width characterize the surfaces of these nanocrystals. The strips can be assigned to lamellae formed of closely packed extended $C_{60}H_{122}$ chains whose length is equal to 7.5 nm. The fact that the lamellar orientations differ by ∼60° implies a correlation between the chain alignment and

(14) Zhong, Q.; Innis, D.; Kjoller, K.; Elings, V. B. *Surf. Sci. Lett.* **1993**, *290*, L688.
(15) Lyubchenko, Y. L.; Jacobs, B. L.; Lindsay, S. M. *Nucleic Acids Res.* **1992**, *20*, 3983.
(16) Ivanov, D. A.; Daniels, R.; Magonov, S. N. *Exploring the High-Temperature AFM and Its Use for Studies of Polymers*; Application Note; Digital Instruments/Veeco Metrology Group: Santa Barbara, CA, 2001. URL: http://di.com/AppNotes_PDFs/AN45%20HeatingStage.pdf.
(17) Ivanov, D. A.; Amalou, Z.; Magonov, S. N. *Macromolecules* **2001**, *34*, 8944.
(18) Tartsch, B.; Moeller, M.; Magonov, S. N. In preparation.
(19) Sikes, H. D.; Schwartz, D. K. *Science* **1997**, *278*, 1604.
(20) Kistenmacher, T. J.; Philips, T. E.; Cowan, D. O. *Acta Crystallogr., Sect. B* **1974**, *30*, 763.
(21) Magonov, S. N.; Cleveland, J.; Elings, V.; Denley, D.; Whangbo, M.-H. *Surf. Sci.* **1997**, *389*, 201.
(22) Percec, V.; Holerca, M. N.; Magonov, S. N.; Yeardley, D. J. P.; Ungar, G.; Duan, H.; Hudson, S. D. *Biomacromolecules* **2001**, *2*, 706.

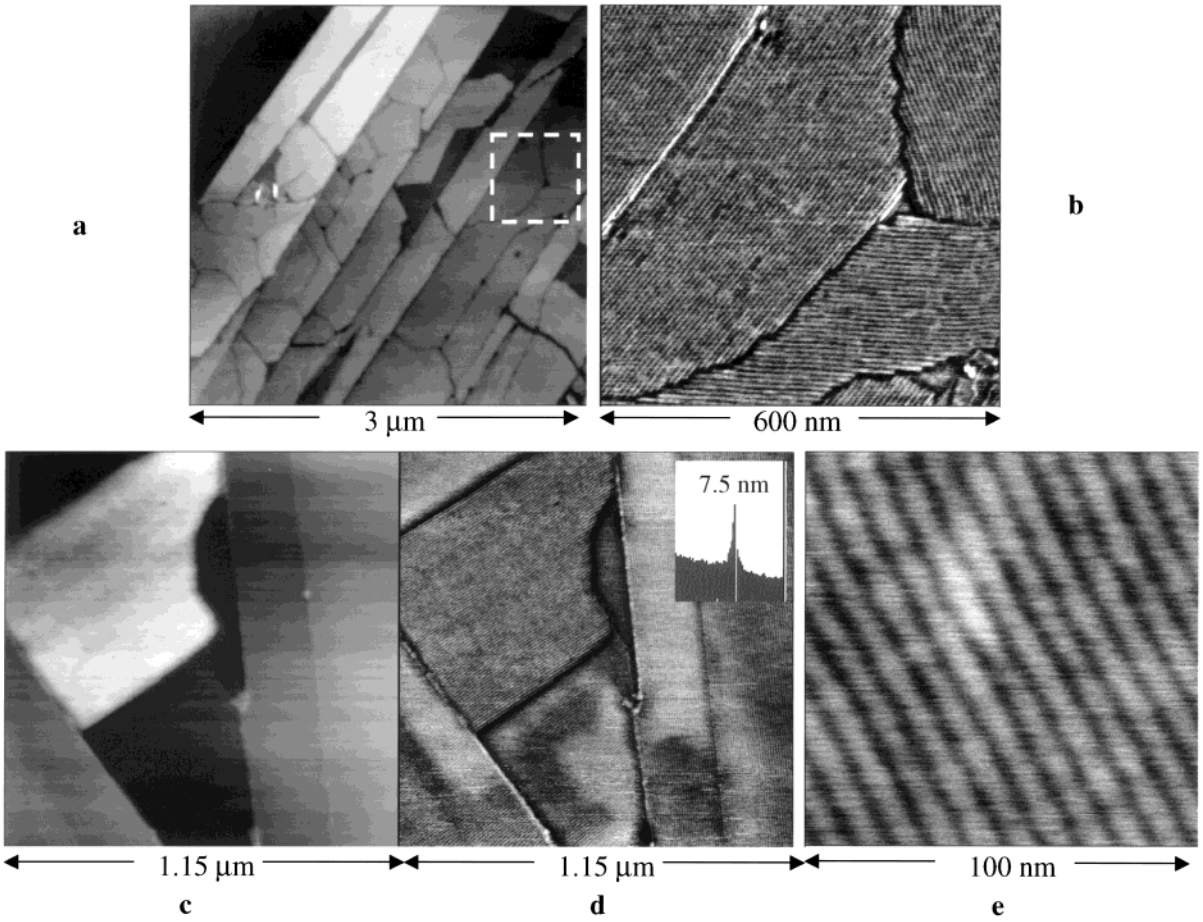

Figure 1. (a) AFM height image of nanocrystals of $C_{60}H_{122}$ alkanes. (b) AFM phase image of the area shown with a square in (a). (c,d) Height and phase AFM images of a single $C_{60}H_{122}$ crystal surrounded by graphite steps. A power spectrum density plot is shown in the insert at the top right corner of the phase image. (e) High-resolution height image, showing lamellae of the epitaxial $C_{60}H_{122}$ layer on graphite.

the graphite lattice, which has 3-fold symmetry. When a sample is prepared from a solution of lower concentration, most of the surface areas are free of the nanocrystals. A single $C_{60}H_{122}$ nanocrystal is shown in Figure 1c. Its height is around 10 nm, and it is higher than most of the other nanocrystals found in the alkane samples. A more typical height is between 3 and 5 nm. The phase in Figure 1d distinctively shows 7.5 nm lamellae not only on the nanocrystal surface but also on surrounding areas. This suggests a lamellar order in $C_{60}H_{122}$ layers lying immediately on the substrate. The high-resolution height image of the lamellar layer on graphite, Figure 1e, shows the alkane lamellae separated by dark rows, which actually represent terminal methyl groups. The latter are more mobile than epitaxial fixed $-CH_2-$ groups that allow an AFM probe to penetrate down to the substrate and emphasize lamellar edges in the height image. Molecular-scale variations in the image contrast (e.g., a bright patch in the top part of the image in Figure 1e) are due either to some adsorbed species on the substrate or to imperfections in the substrate. In tapping mode imaging, we have not been able to resolve individual alkane chains as has been done with STM.[3]

A series of AFM images were obtained at different temperatures on a surface area, which is shown in the height image obtained at room temperature, Figure 2a. We have monitored the structural changes of this location at elevated temperatures. Particularly, we have measured the height of one nanocrystal (marked with an arrow in the top part of the image), which is 2.8 nm at room temperature. This height did not change in the images recorded at 80 °C, Figure 2b,c. After the image was recorded at 80 °C, Figure 2b, a smaller area (700 nm on side) in the center was imaged at the elevated tip-force, and the lamellar structures of 7.5 nm in width have been seen in the high-force image (not shown here). The low-force image obtained afterward, Figure 2c, shows a window indicating that an area of the crystals in the center was removed. This means that the nanocrystals are composed of multiple lamellar layers and that the removed alkane material does not appear in the image. Most likely, disordered traces of this material are scattered on the surface weakly bound to it or they are dispersed in a liquid contamination layer, which is always present on surfaces in air. When we continued the low-force scanning of the same area at 85 and 90 °C, the window became shallow and almost disappeared at 90 °C (Figure 2d). Remarkably, at these temperatures the height of the nanocrystal in the top part of the area is only 0.5 nm. Therefore, at temperatures approaching the T_m of bulk $C_{60}H_{122}$ crystals thermal and mechanical stability of the nanocrystals becomes inferior and thickness of the nanocrystals is drastically reduced. Such partial melting might occur simultaneously with crystallization, which can explain the emergence of new surface nanocrystals in the left side of the area in Figure 2d. Further heating of the sample to 95 and 100 °C led to complete melting of the nanocrystals. Only a few nanocrystals remained in the left part of the image recorded at 95 °C, Figure 2e. At 100 °C, the surface area is completely free from nanocrystals as seen in the height image in Figure 2f. Strips of different shape and size, which are visible in this image, are

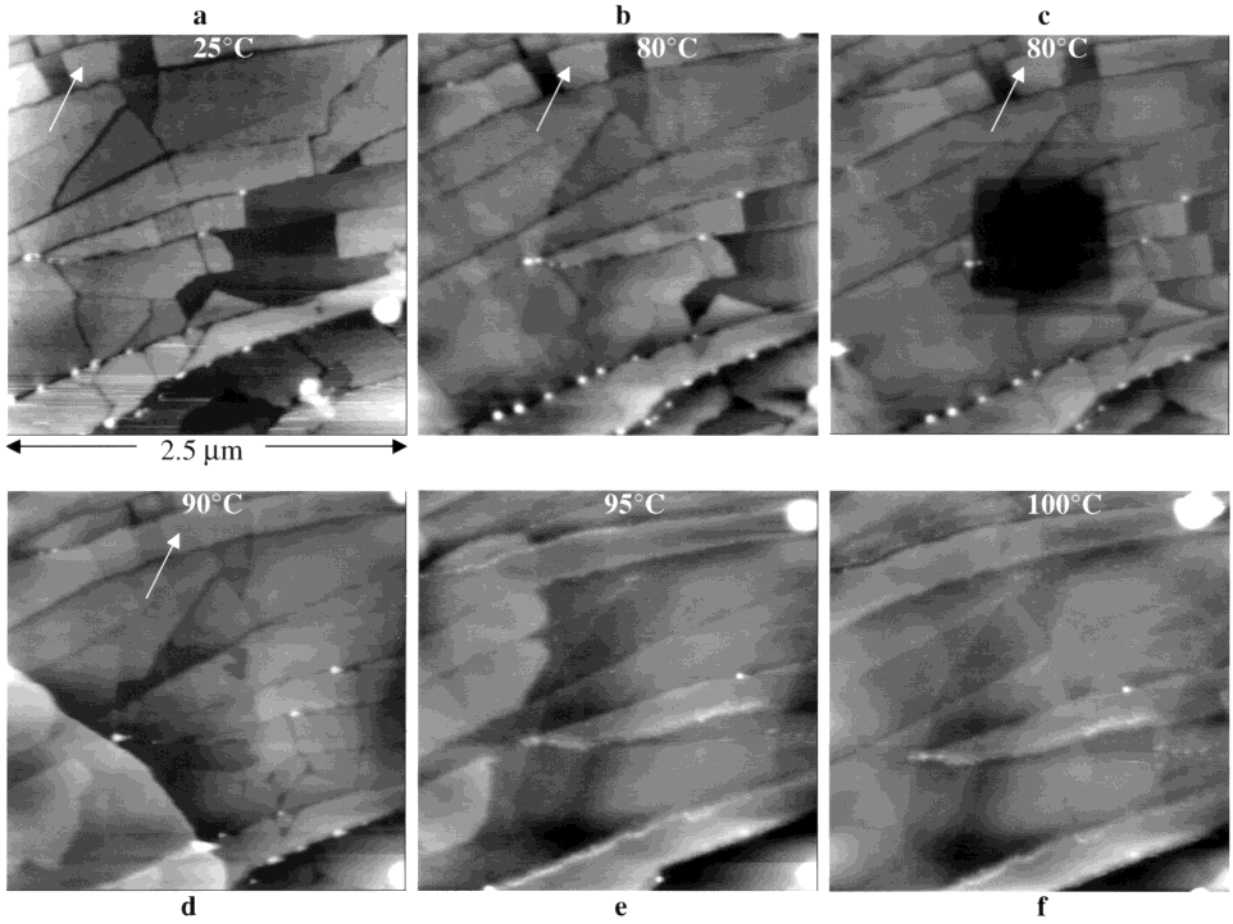

Figure 2. (a−f) AFM height images of the same area of the $C_{60}H_{122}$ film, which are taken at different temperatures. The image in (c) was recorded after high-force scanning in the center of the area. The arrows indicate a nanocrystal, whose height was measured from the cross-sectional profiles.

imperfections of the graphite surface that appeared after cleavage of the substrate.

Though the nanocrystals melt at temperatures close to the bulk melting temperature, the epitaxial layers are more thermally stable. The epitaxial layers cover the graphite areas, and the lamellar structures of these layers have been observed at temperatures up to 140 °C as shown in Figures 3 and 4. The phase images, which were recorded on the epitaxial alkane layer at 130 °C, show various domains with differently oriented lamellae, Figure 3a,b. Remarkably, the lamellar orientation of one of the domains, which is marked with an arrow, has changed. Most likely, the lamellar reorientation is invoked by increased molecular mobility, as it was not observed at lower temperatures (100 and 120 °C). Heating of the alkane samples from 130 to 140 °C induced the lamellar reorientation of two domains in a location shown in Figure 4a,b. The lamellae were no longer seen after the sample temperature was raised from 140 to 145 °C. When the sample temperature is lowered to 140 °C, epitaxial order is restored. The reorientation of lamellae was found after cooling of the sample to 90 °C. The power spectrum density plots, which are also placed above the images, show that there are no noticeable changes in the lamellar width (7.4−7.5 nm) at elevated temperatures.

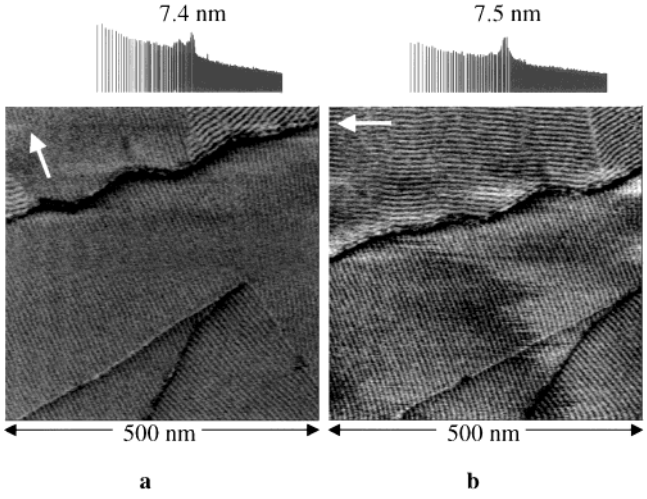

Figure 3. (a,b) Two sequential AFM phase images of an epitaxial $C_{60}H_{122}$ film at 130 °C. Power spectrum density plots are shown above the images. White arrows indicate that an orientation of the lamellae epitaxially covered the same graphite domain.

Discussion

In our experiments, tapping mode AFM was applied to study structural organization of ultrathin $C_{60}H_{122}$ alkane layers on graphite. We found that spin-casting of the alkane solution on graphite leads to the formation of epitaxial lamellar layers and nanocrystals. In the lamellae, the alkane molecules, which are aligned along the main crystallographic directions of the substrate, are oriented perpendicular to the lamellar edges. Despite the well-defined orientation of normal alkanes on the graphite shown in AFM images (which is even better revealed in

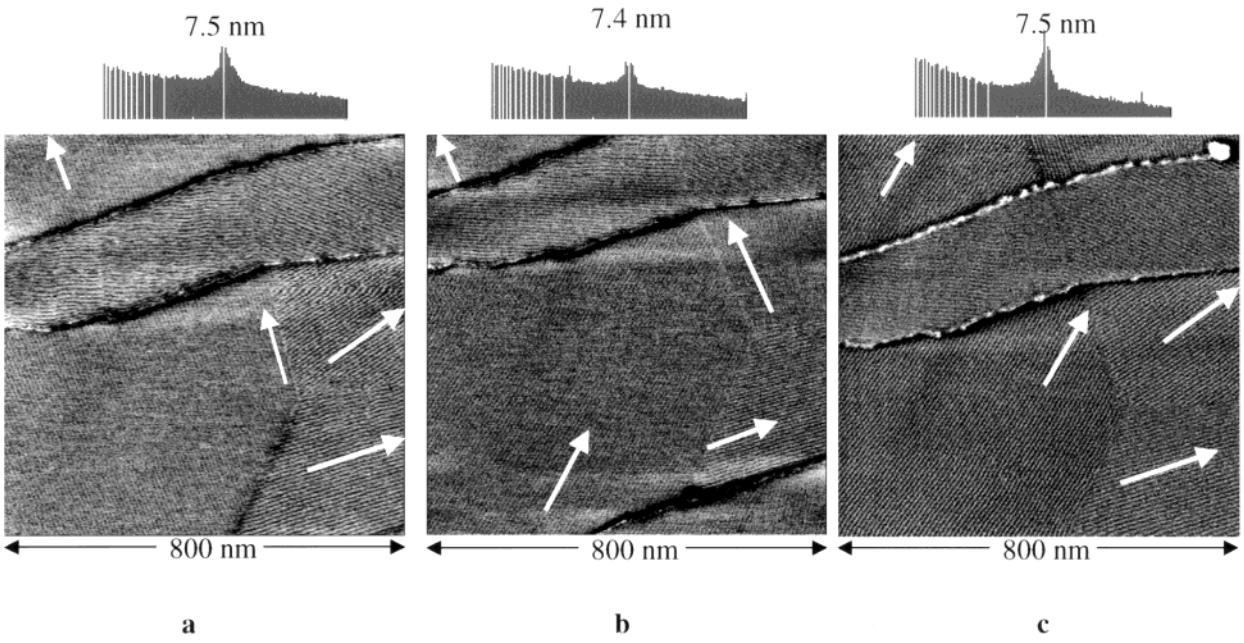

Figure 4. (a−c) AFM phase images of an epitaxial $C_{60}H_{122}$ film at 130, 140, and 90 °C, respectively. Power spectrum density plots are shown above the images. White arrows indicate lamellar orientation in different graphite domains.

STM images made at the liquid−graphite interface[3,4]), it is rather difficult to come up with the unique molecular-scale model of alkane arrangement on graphite. This is not only because of the possible alkane tumbling[4,7] on graphite but also because of the fact that lamellar order of alkane layers was also observed on other layered crystals such as MoS_2[23] and WSe_2.[24] The latter crystals exhibit atomically flat surfaces with hexagon packing characterized by 0.32 nm spacing in contrast to 0.25 nm spacing of the surface honeycomb pattern of graphite. It looks like an exact match between the repeat distance along the alkane chain (0.25 nm in the all-trans conformation), and the lattice parameter of the substrate is not needed for such an arrangement.

The nanocrystals, which are formed of multiple lamellar sheets with the alkane molecules oriented parallel to the substrate, are an example of homoepitaxy. Though melting of the nanocrystals around the melting temperature of bulk $C_{60}H_{122}$ crystals can be expected, the ability of the AFM probe to penetrate through the alkane melt allows the revealing of the epitaxial alkane layer on the substrate. This epitaxy is preserved at temperatures at least 45° higher than the melting temperature of the bulk crystals. This phenomenon has a more general character. Our preliminary data on high-temperature AFM studies of an ultralong alkane $C_{390}H_{782}$ layer on graphite show that the epitaxy is preserved at temperatures up to 180 °C.[25]

The epitaxial alkane layers and the nanocrystals can be used as a calibration standard for lateral AFM measurements in the sub-100-nm scale. Piezoceramic actuators, which are used in AFM microscopes, are known for their nonlinear behavior. Therefore, the actuator calibration is an essential part of microscope use. At present, the microfabricated gratings, which are applied for this purpose, have dimensions in the scale of hundreds of nanometers. “Natural” standards such as the epitaxial $C_{60}H_{122}$ layers or their nanocrystals with the spacing of 7.5 nm are viable candidates for such calibration. AFM imaging of these layers is easier than that of molecular crystals (e.g., TTF/TCNQ; see the Experimental Section). The last hurdle is related to the assumption that the alkane chains are oriented perpendicular to the lamellar edges. Such an assumption looks rational, but its final proof can be provided by molecular-resolved images of the $C_{60}H_{122}$ layers, which might be obtained with STM (at room temperature or at elevated temperatures) or with contact AFM mode. These studies are in progress.

LA0206615

(23) Cincotti, S.; Rabe, J. P. *Appl. Phys. Lett.* **1993**, *62*, 3531.
(24) Magonov, S. N. Unpublished data.
(25) Magonov, S. N.; Yerina, N.; Ungar, G.; Ivanov, D. In preparation.